© 1997 The Chemical Society of Japan

Steric-Hindrance Effect of a Substituent in the Self-Assembly Process of Copper(II) Complexes with Quadridentate Schiff-Base Ligands Involving a 2-Substituted-Imidazole Moiety

Naohide Matsumoto,* Masaaki Mimura, Yukinari Sunatsuki, Shingo Eguchi,† Yukiko Mizuguchi,† Hitoshi Miyasaka,† and Toshio Nakashima††

Department of Chemistry, Faculty of Science, Kumamoto University, Kurokami 2-39-1, Kumamoto 860

†Department of Chemistry, Faculty of Science, Kyushu University, Hakozaki, Higashi-ku, Fukuoka 812

††Faculty of Education, Oita University, Dannoharu 700, Oita 870-11

(Received May 6, 1997)

Four copper(II) complexes with unsymmetrical quadridentate ligands involving an imidazole moiety, $[CuHL^n]ClO_4$ (**1**—**4**; $n=1$—4), have been prepared and characterized, where HL^1 = *N*-salicylidene-*N*′-(2-methylimidazol-4-ylmethylidene)-1,3-propanediamine, HL^2 = *N*-salicylidene-*N*′-(2-phenylimidazol-4-ylmethylidene)-1,3-propanediamine, HL^3 = *N*-acetylacetonylidene-*N*′-(2-methylimidazol-4-ylmethylidene)ethylenediamine, HL^4 = *N*-acetylacetonylidene-*N*′-(2-phenylimidazol-4-ylmethylidene)ethylenediamine, respectively. The corresponding deprotonated complexes **1′**—**4′** were obtained when **1**—**4** were treated under an alkaline condition. Deprotonation of the imidazole moiety of the copper(II) complex motivates a self-assembly process which is formed by an axial coordination of the imidazolate nitrogen atom of a molecular unit to the copper(II) ion of another unit. **1′**—**3′** assumes a self-assembled imidazolate-bridged infinite-chain structure $\{Cu(II)\text{–}Im\}_n$ in the solid state, while the polymeric species dissociates to monomeric species in the solution state. **4′** consists of a discrete deprotonated monomeric species, even in the solid state. The physical measurements, including reflectance and absorption spectra, cryomagnetic measurements, and single-crystal X-ray analyses, revealed that the self-assembly behavior for the series of copper(II) complexes depends both on the steric effect of the substituent of 2-substituted-4-formylimidazole moiety and the ligand field strength of the equatorial quadridentate ligand.

A self-assembly process involving metal ions has attracted much attention in the field of supramolecular chemistry from the viewpoints of the construction of single- or double-helical and catenated structures and the development of functional materials with new concepts.[1,2] A metal ion can be useful for a self-assembling process, because a metal ion together with a ligand contains a variety of structural information to guide the self-assembly reaction,[1—3] J. -M. Lehn and co-workers reported an unique double- and triple-helical structures comprising metal ions and oligobipyridine ligands, in which the supramolecular structure, a so-called helicate, results from the formation of coordination bonds between the metal ions and oligobipyridine ligands, and the combination of the coordinating geometry around the metal ions and the structural shape of the oligo-bidentate strand ligand results in its helical structure.[4,5]

As a further development of this fascinating area of supramolecular chemistry, metal complexes reversibly interconverting between monomers and self-assembled oligomers by the input of external information would be of utmost interest. From this point of view, we have attempted to design a self-assembly system in which a reversible conversion between monomers and their self-assembled oligomer or polymer is available, depending on the pH.[6] We have reported that metal(II) complexes with the multidentate Schiff-base ligand involving an imidazole moiety per complex undergo a dessociation of the imidazole proton to give a cyclic oligomer (tetramer or hexamer) and an unique helical or zigzag-chain polymer, depending on the ligand system and metal ion; also, the reverse process from oligomer or polymer to monomers is also available due to the protonation.[6] This type of metal complex itself behaves like a simple building block for the self-assembly process, and exhibits the following characteristics:[6,7] (1) The complex has a potential donor coordination ability at the imidazolate nitrogen atom. (2) The complex has a potential acceptor coordination ability at the vacant or substitutable coordination site. (3) Although the complex potential has both donor and acceptor coordination abilities, the donor ability is absent and the complex exists as a monomer when the proton associated with the imidazole nitrogen under a pH region lower than pK_H. When the proton dissociates under a pH region higher than pK_H, the donor coordination ability appears at the imidazolate nitrogen atom and the self-assembly process would be motivated. In this system, a construction process from isolated monomeric molecules to the assembled oligomeric or polymeric molecule and the reverse deconstruction process are both available by adjusting the pH as external information.

(4) The resulting self-assembled molecular structure should be determined cooperatively, depending on the ligand framework and the metal ion, because the ligand framework can give a steric restriction and the metal ion assumes its preferable coordination geometry.

There are many ways to control the characteristics in the self-assembly process. When the discussion is limited to copper(II) complexes with planar quadridentate ligands, as given in Scheme 1, one way is to control the ligand-field strength of the metal complex, in which the acceptor ability at the axial coordination site can be controlled indirectly by the ligand field of the equatorial ligand, as described previously.[6)] Another way to control the assembly property is to use a steric effect. The introduction of a bulky substituent at the 2-position of the imidazole moiety of the precursor building block prevents the self-assembly process, because the coordination of the imidazolate nitrogen atom to the metal ion of the adjacent unit may be prohibited sterically. In order to investigate the steric-hindrance effect as well as the ligand-field effect, we synthesized two series of copper(II) complexes with quadridentate Schiff-base ligands involving a 2-substituted-imidazole moiety per complex, whose chemical structures and abbreviations given in Scheme 1. In this paper, the syntheses, characterization, and structures of the protonated copper(II) complexes **1**—**4** and the deprotonated complexes **1′**—**4′** are reported.

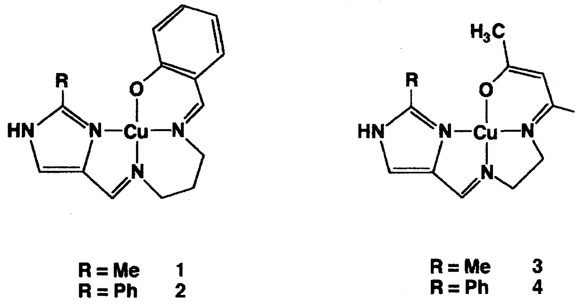

1: [Cu(HL^1)]$^+$, 2: [Cu(HL^2)]$^+$, 3: [CuHL^3]$^+$, 4: [CuHL^4]$^+$

Scheme 1. Structures of four protonated copper(II) complexes and the abbreviations. The deprotonated complexes are abbreviated as **1′**—**4′**.

Results and Discussion

Synthesis and Characterization of Protonated Complexes 1—4 and Deprotonated Complexes 1′—4′. The protonated copper(II) complexes **1**—**4** can be prepared by two methods, method (1) and method (2). Method (1) involves half-unit ligands, *N*-aminopropylsalicylaldimine and *N*-acetylacetonylideneethylenediamine, which are first prepared according to the procedures of Elder[8)] and Costes,[9)] respectively. Secondly unsymmetrical quadridentate ligands, HL^n ($n = 1$—4), are prepared by a condensation reaction of the half-unit ligands and 2-substituted-4-formylimidazole in methanol; finally, the copper(II) complexes are prepared by the reaction of quadridentate ligands and copper(II) nitrate or copper(II) perchlorate. Method (2) involves copper(II) complexes of the half-unit ligands HL′ with the formula, [CuL′(py)]ClO$_4$ or [CuL′(ac)] (py = pyridine, ac = acetate), which are prepared by a method of Costes;[10)] then, the reaction of the complex and 2-substituted-4-formylimidazole in methanol gives the copper(II) complexes with the unsymmetrical quadridentate ligands. The IR spectra of these complexes have shown the characteristic bands assigned to the C=N stretching vibration of a Schiff-base at 1600—1650 cm^{-1}, the imidazole N–H vibration at 3150—3250 cm^{-1}, and the counter anion (NO$_3^-$: ca. 1400 cm^{-1}, ClO$_4^-$: ca. 1100 cm^{-1}),[11)] where the IR bands due to the imidazole N–H and the counter anion are indicative of the protonated form of these complexes. The molar electrical conductivities measured in ca. 10^{-3} mol dm^{-3} methanol solutions are in the expected range of the 1 : 1 electrolytes,[12)] as given in Table 1.

Deprotonated copper(II) complexes, **1′** and **2′**, were isolated as bright-green crystals by the addition of excess triethylamine to a methanol solution of the corresponding protonated complexes, **1** and **2**, respectively. This method is not useful for the syntheses of **3′** and **4′**, since **1′** and **2′** are moderately soluble in methanol, but **3′** and **4′** are very soluble in methanol. An alternative procedure for syntheses of the deprotonated complexes, **3′** and **4′**, is as follows. The protonated complexes are suspended in a mixture of chloroform/water (1/1 in the volume), and to the suspension

Table 1. The d–d Band Maxima of the Diffuse Reflectance and Absorption Spectra, Together with the Colors, Molar Electrical Conductivities, and Melting Points

Complexes	λ_{max}/nm Solid state	Color	λ_{max}/nm (ε/dm^3 mol^{-1} cm^{-1}) MeOH	Color	Λ_M/S cm^2 mol^{-1} MeOH	CHCl$_3$	Mp/°C
1	576	Olive green	593 (98)	Green	90	—	246
2	540	Olive yellow	601 (93)	Yellow green	94	—	>280 (decomp)
3	528	Dark red purple	549 (195)	Violet	103	—	220
4	567	Dark violet	567 (229)	Blue	107	—	>280 (decomp)
1′	653	Bright green	589 (87)	Yellowish green	42	0	256
2′	656	Bright green	598 (91)	Yellow green	43	0	249
3′	632	Blue green	546 (196)	Purple	49	0	155
4′	566	Dark violet	565 (209)	Blue	40	0	207

The protonated complexes **1**—**4** are insoluble in CHCl$_3$. The electrical conductivities of **1′**—**4′** in CHCl$_3$ are zero within the experimental error.

is added an equivalent amount of aqueous solution of 1 M NaOH (1 M = 1 mol dm^{-3}). After the mixture is stirred for ten min., the chloroform layer is collected and evaporated to nearly dryness at room temperature to give deprotonated complexes **3′** (blue green) and **4′** (dark violet). The characteristic IR bands due to the imidazole N–H vibration and the corresponding counter anion observed in their precursor protonated compounds are absent in the spectra of **1′**—**4′**. The electrical conductivity in chloroform is nearly equal to zero, indicating that the deprotonated complexes are electrically neutral in chloroform. However, it should be noted that the electrical conductivities for **1′**—**4′** measured in methanol are around 45 S cm^2 mol^{-1}, whose value is nearly half that of the 1 : 1 electrolyte.

Structural Description of Protonated Complexes 1, 3, and 4. ORTEP drawings of the cationic complex for **1**, **3**, and **4** with the atom numbering schemes are shown in Fig. 1. Each of the crystals consists of the protonated copper(II) complex with the unsymmetrical quadridentate ligand derived from the 1 : 1 : 1 condensation product of salicylaldehyde (or acetylacetone), 1,3-propanediamine (or ethylenediamine), and 2-substituted-4-formylimidazole, and a perchlorate ion as the counter anion. A packing diagram of **4** is given in Fig. 2, showing that the copper(II) ion assumes a square-planar coordination geometry with the N_3O donor atoms of the quadridentate Schiff-base ligand, and that the perchlorate anion does not coordinate to the cooper(II) ion, but is hydrogen bonded to the imidazole nitrogen atom with O···N distance of 2.906(5) Å; **3** assumes a similar crystal structure consisting a discrete mononuclear copper(II) complex and a perchlorate anion with a hydrogen bond of 2.88(1) Å. On the other hand, **1** assumes a binuclear structure bridged by two phenoxo oxygen atoms in out-of-plane fashion, where Cu–O(1) and Cu–Cu distances of 2.892(5) and 3.673(2) Å, respectively, are considerably long. One of the oxygen atoms of the perchlorate ion is hydrogen-bonded to the imidazole nitrogen with a distance of 2.88 (1) Å.

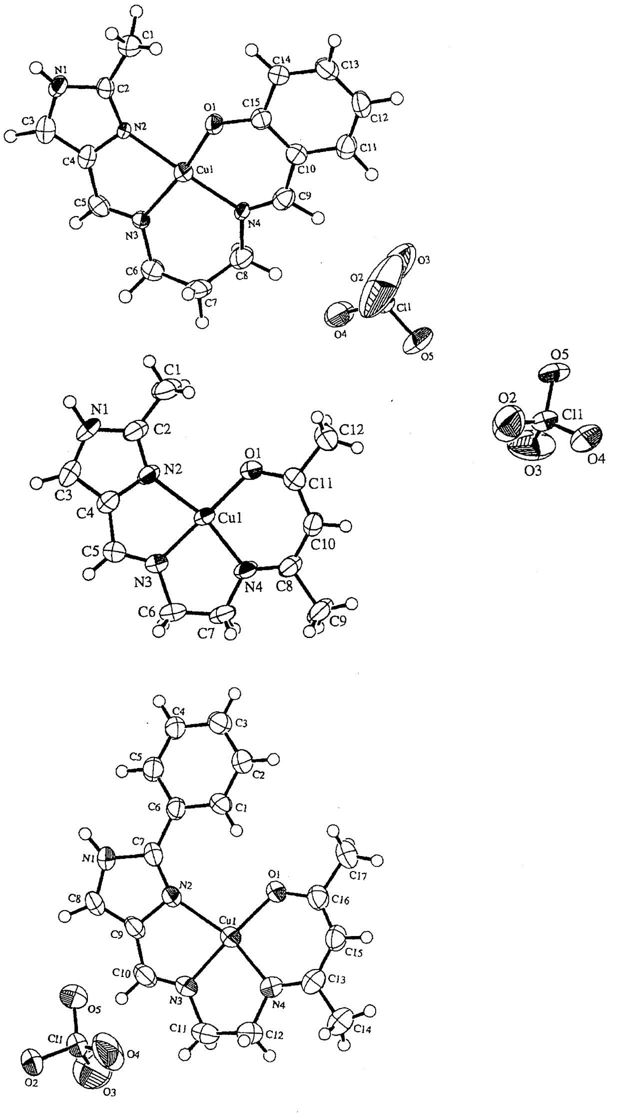

Fig. 1. ORTEP drawings of the cationic complexes for **1**, **3**, and **4** with the atom numbering scheme, showing their unique units and 50% probability ellipsoids.

Structural Description of $[CuHL^2][Cu(saltn)]ClO_4$. In the course of the synthesis of **2**, a compound with the chemical formula of $[CuHL^2][Cu(saltn)]ClO_4$ was obtained as a subproduct. An ORTEP drawing of $[CuHL^2][Cu(saltn)]ClO_4$ with the atom numbering scheme and the edge-on view of the cationic binuclear molecule are given in Fig. 3(a) and (b), respectively. The crystal consists of a cationic binuclear molecule and a perchlorate anion. The binuclear complex assumes a phenoxo-bridged binuclear structure of an out-of-plane fashion, in which one of two phenoxo oxygen atoms of Cu(saltn), O(2), coordinates to Cu(1) of $CuHL^2$ as the fifth donor atom at a distance of 2.456(8) Å, and the pheno oxygen atom O(1) of $CuHL^2$ interacts with Cu(2) of Cu(saltn) at a distance of 2.611(9) Å, which is slightly long for axial coordination.

Structural Description of Deprotonated Complex 2′. An ORTEP drawing of unique molecules of **2′** with the atom numbering scheme is shown in Fig. 4. An one-dimensional

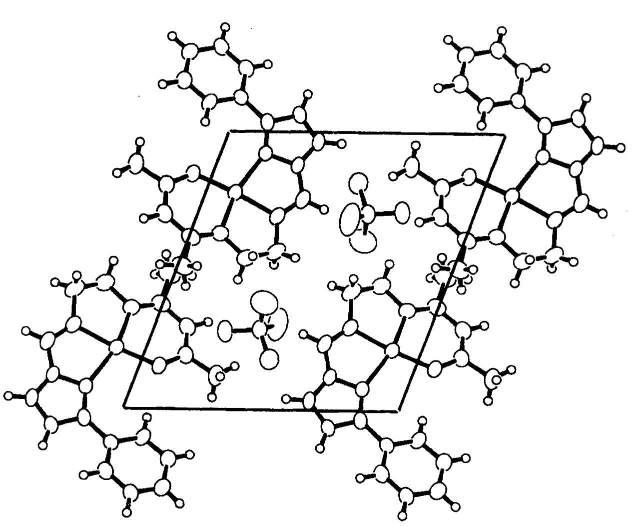

Fig. 2. A packing diagram of **4** consisting of a cationic complex $[CuHL^4]^+$ and a perchlorate anion.

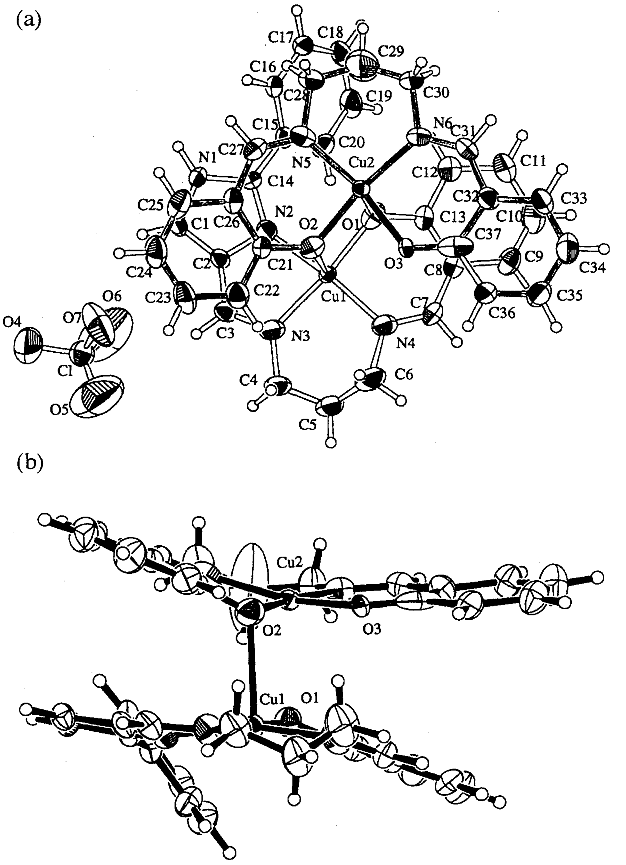

Fig. 3. (a) An ORTEP drawing of $[CuHL^2][Cu(saltn)]ClO_4$ with the atom numbering scheme, showing 30% probability ellipsoids. (b) An edge-on view representing an axial coordination bond of Cu(1)–O(2) = 2.456(8) Å and a weak interaction of Cu(2)–O(1) = 2.611(9) Å.

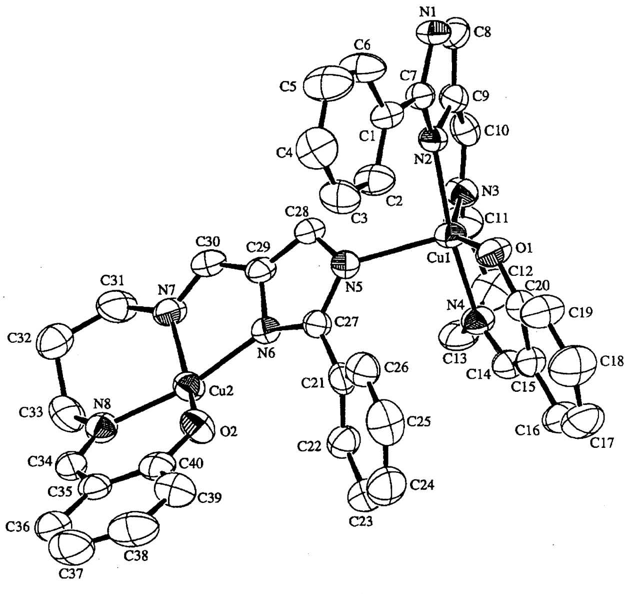

Fig. 4. An ORTEP drawing of **2′** with the atom numbering scheme, showing the unique unit and 50% probability ellipsoids.

helical-chain structure running along the *b*-axis is shown in Fig. 5.

The asymmetrical unit of **2′** consists of two molecular units bridged by an imidazolate group; these symmetric units are connected through intermolecular imidazolate bridges by a symmetry operation of a two-fold screw axis along the *b*-axis. There are two crystallographically independent Cu(II) ions, Cu(1) and Cu(2), in the crystal, and each copper(II) ion assumes a square-pyramidal coordination geometry in which the basal coordination plane is occupied by N_3O donor atoms of the quadridentate ligand and the apical site is occupied by an imidazolate nitrogen atom. Cu(1) is coordinated axially by the intramolecular imidazolate nitrogen atom N(5), with a Cu–N distance of 2.228(6) Å, and Cu(2) is coordinated by the nitrogen atom, $N(1)^*$, of an adjacent unit with a Cu–N distance of 2.461(6) Å. The bond distances of the axial coordination, 2.228(6) and 2.461(6) Å, are substantially different, probably due to the steric effect of the phenyl group. They are compared with the average distance of 2.230 Å reported for (*N*-salicylidene-*N′*-imidazolato-4-ylmethylene-1, 3-propanediamino)copper(II)[6c] and 2.162(6) Å of (*N*-3-ethoxysalicylidene-*N′*-imidazolato-4-ylmethylenecyclohexane-1,2-diamino)copper(II).[6b] It should be noted that **2′** is moderately soluble in methanol, and two compounds reported previously are insoluble in methanol, and even in DMF. The solubility for these complexes can be rationalized by the difference of the distance in the coordination bond of copper-imidazolate nitrogen.

Structural Description of 4′. An ORTEP drawing of **4′** with the atom numbering scheme is shown in Fig. 6. A packing diagram of the molecules in the crystal is shown in Fig. 7. The crystal consists of a discrete electronically neutral $[CuL^4]$ species stacked parallel in the crystal; there is no axial coordination between the molecules, as shown in Fig. 7. The copper(II) ion assumes a square-planar coordination geometry with the N_3O donor atoms of the quadridentate ligand, and the average distance of the Cu–N and Cu–O bonds is 1.963 Å. This value is compatible with the corresponding value, 1.963 Å, of the protonated complex **4**, but slightly longer than the protonated complexes involving acetylacetone residue (1.942 Å).[7b]

Effect of Bond Distances of Cu-Equatorial Ligand and Cu-Axial Ligand on the Self-Assembly Property. The coordination-bond distances and the averaged value for the protonated and deprotonated complexes, together with those of the related complexes reported previously,[6] are summarized in Table 2. The average bond distances of the protonated complexes consisting of the salicylaldehyde moiety are in the range of 1.963—1.978 Å, and those of complexes consisting of acetylacetone moiety are in the range of 1.940—1.963 Å, indicating that the former complexes denoted as A assume a weaker equatorial ligand field than the latter denoted as B. Under the deprotonation procedure, A precipitates a self-assembly species more immediately than B, and gives much more stable and insoluble species than B, because it is expected that the axial coordination bond distance of A is shorter than that of B.

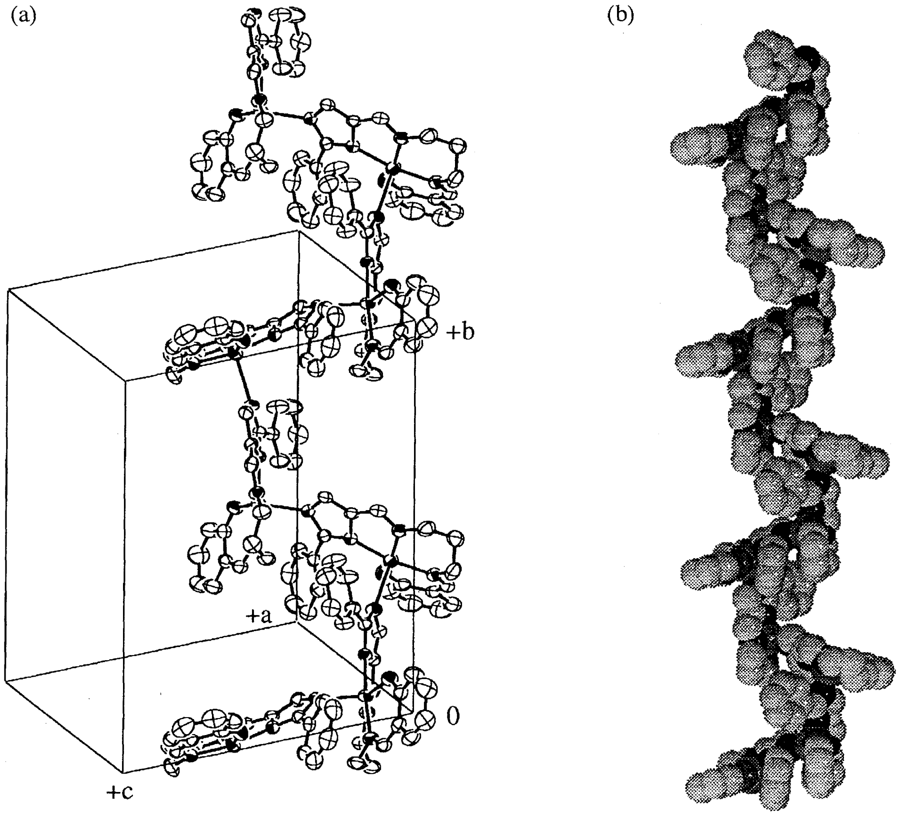

Fig. 5. An one-dimensional helical structure of **2′** running along the *b*-axis. (a) ORTEP drawing. (b) space filling model.

It is generally accepted for the square pyramidal copper(II) complex, that the shorter is the distance of Cu-equatorial ligand, the longer is the distance of Cu-axial ligand, though the discussion is limited to within a similar ligand system. The relation between the distances of the Cu-axial ligand and the Cu-equatorial ligand can be experimentally examined by **2′**, which contains two crystallographically independent copper sites, Cu(1) and Cu(2). The average distance, 2.005 Å, of the equatorial ligand for Cu(1) is longer than the corresponding value, 1.975 Å, for Cu(2); on the contrary, the Cu–N(axial) distance of 2.228(6) Å for Cu(1) is shorter than 2.461 Å for Cu(2). A comparison of a square-planar protonated complex **a** with a square-pyramidal deprotonated complex **a′** would give additional evidence for the correlation, where **a** denotes (*N*-(salicylidene)-*N*′-(imidazolylmethylidene)-1,3-propanediamino)copper(II) and **a′** denotes the deprotonated complex. The average distances of the equatorial ligand for **a** and **a′** are 1.973 and 1.988 Å, respectively, indicating that the axial coordination with Cu–N = 2.230 Å elongates the distance of the equatorial coordination sphere.

Magnetic Properties of Deprotonated Complexes 1′—4′. The cryomagnetic susceptibilities were measured in order to investigate the magnetic interaction of the self-assembled structure. The magnetic behavior of **1′** is shown in Fig. 8 in the forms of plots of $1/\chi_A$ vs. *T* and μ_{eff} vs. T, where χ_A is the magnetic susceptibility per copper(II) ion, μ_{eff} is the effective magnetic moment, and *T* is the absolute temperature. The μ_{eff} of complex **1′** at room temperature is 1.86 μ_B, which is slightly larger than the spin-only value expected for $S = 1/2$, and μ_{eff} gradually increases to 2.00 μ_B at 4.3 K upon lowering the temperature. The inverse of the magnetic susceptibility obeys the Curie–Weiss law with Weiss constant of +1.5 K. On the other hand, the inverse of the magnetic susceptibility for **2′**, **3′**, and **4′** obeys the

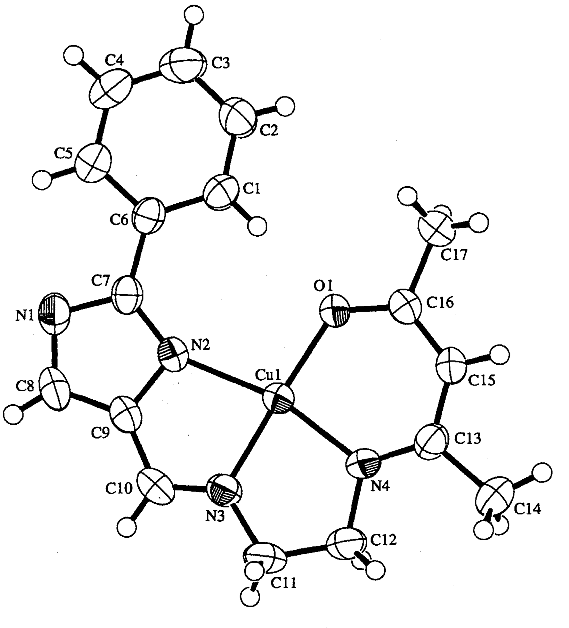

Fig. 6. An ORTEP drawing of **4′** with the atom numbering scheme, showing the unique unit and 50% probability ellipsoids.

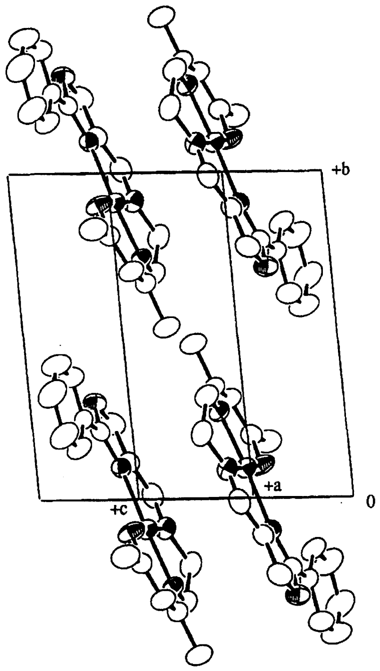

Fig. 7. A packing diagram of **4′**, showing a parallel packing of the planar molecules and representing no intermolecular coordination bonding.

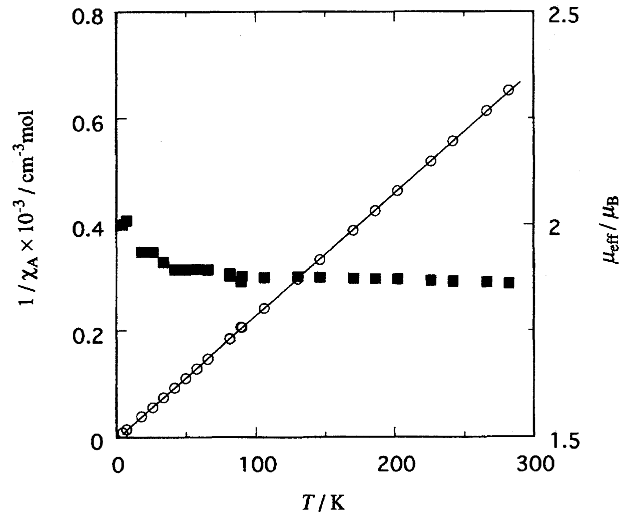

Fig. 8. Temperature dependence of the inverse of the magnetic susceptibility and effective magnetic moment per copper for **1′**.

Curie–Weiss law with negative Weiss constants of −30.2, −5.1, and −9.5 K, respectively, where the magnetic susceptibility was measured in the temperature range from liquid-nitrogen temperature to room temperature; also, it should be noted that an imidazolate-bridged zigzag-chain structure and an isolated monomeric structure have been confirmed by X-ray analyses for **2′** and **4′**, respectively. The effective magnetic moments of 1.90, 1.87, and 1.83 μ_B at room temperature for **2′**, **3′**, and **4′** decrease to 1.74, 1.81, and 1.77 μ_B, at 78 K, respectively. These magnetic data demonstrated that the magnetic interaction for a series of deprotonated complexes is weak, regardless of the ferromagnetic and antiferromagnetic interaction. These results are compatible with those of deprotonated complexes without the substituent of the imidazole moiety (*N*-salicylidene-*N′*-(imidazolato-4-ylmethylidene)-1,3-propanediamine)copper(II)[7c] and (*N*-3-ethoxysalicylidene-*N′*-imidazolato-4-ylmethylidene)-*trans*-1,2-cyclohexanediamino)copper(II),[7d], in which an infinite-chain structure bridged by an imidazolate group is confirmed by X-ray analyses and the Ising model[13] with the spin Hamiltonian in the form $H=-2\sum J_{ij}S_iS_j$ was used to give the best-fit parameters of $J=-15$ ($\theta=-25$ K) and -1.8 ($\theta=-8.5$ K) cm^{-1}, respectively. The weak magnetic interaction, either ferromagnetic and antiferromagnetic, can be rationalized by an almost perpendicular orientation of the adjacent two

Table 2. Cu–N, Cu–O Distances (Å) for the Protonated and Deprotonated Complexes

Compound	Cu–O(1)	Cu–N(2)	Cu–N(3)	Cu–N(4)	Averaged value	
(1) Distances of the protonated compounds						
1	1.903(5)	2.023(6)	2.018(6)	1.967(6)	1.978	A[b)]
3	1.886(6)	2.009(6)	1.938(7)	1.936(6)	1.942	B
4	1.866(3)	2.114(4)	1.936(4)	1.937(4)	1.963	B
a[6c)]	1.910(5)	1.951(5)	2.038(6)	1.993(5)	1.973	A
b[6d)]	1.897(6)	1.984(7)	2.036(7)	1.934(7)	1.963	A
c[7b)]	1.881(3)	2.004(3)	1.959(3)	1.925(3)	1.942	B
d[6d)]	1.894(7)	1.980(12)	1.970(9)	1.915(12)	1.940	B
(2) Distances of the deprotonated compounds						
a′[6c)]	1.934	1.987	2.052	1.978	1.988	2.230[a)]
2′	1.932(5)	2.051(6)	2.059(6)	1.977(6)	2.005	2.228(6)[a)]
	1.902(5)	1.995(6)	2.038(6)	1.964(6)	1.975	2.461(6)[a)]
4′	1.874(2)	1.904(2)	1.928(2)	1.956(2)	1.963	—

a; (*N*-salicylidene-*N′*-(imidazolylmethylidene)-1,3-propanediamino)copper(II). **b**; (*N*-(5-bromosalicylidene)-*N′*-(imidazolylmethylidene)-1,3-propanediamino)copper(II). **c**; (*N*-acetylacetonylidene-*N′*-(imidazolylmethylidene)ethylenediamino)copper(II). **d**; (*N*-benzoylacetonylidene-*N′*-(imidazolylmethylidene)ethylenediamino)copper(II). **a′** denotes the deprotonated compound of **a**. The Unsymmetric unit of the crystal comprises three copper units whose geometries are very similar to each other in the distances. a) Cu–N(axial) distance. b) A and B denote the complexes involving salicylaldehyde moiety and acetylacetone moiety, respectively.

copper(II) coordination planes, because the magnetic orbitals are almost orthogonal to each other in such a case. Thus, the magnetic orthogonality leads to a small ferromagnetic interaction, and a slight deviation from a perpendicular orientation would cause an antiferromagnetic contribution.[14)]

Steric and Ligand-Field Effects in the Self-Assembly Process. The diffuse reflectance spectra of polycrystalline samples and the absorption spectra in methanol solutions for the protonated and deprotonated complexes were measured. The d–d band maxima together with their colors, the molar electrical conductivities, and the melting points are given in Table 1. Since in the case of copper(II) complexes with a planar quadridentate ligand, only the axial coordination site is available to assemble the species, the self-assembled structure might be limited to an imidazolate-bridged $\{-\mathrm{Cu(II)}-\mathrm{Im}\}_n$ linear chain structure, unless the planar ligand structure is deformed. Therefore, a physical technique to observe the coordination number would be useful for studying the self-assembly process. The d–d band maxima are indicative of the coordination geometry and the ligand field strength. The d–d band maxima of the protonated complexes in the solid states **1**—**4** are 576, 540, 528, and 567 nm, respectively, and the corresponding deprotonated complexes **1′**—**4′** are 653, 656, 632, and 566 nm, respectively. Except for **4** and **4′**, the d–d band maxima of the protonated compound (528—576 nm) were observed in a shorter wave length than those of the corresponding deprotonated compound (632—656 nm), indicating that the protonated compounds assume a four-coordinated square-planar coordination geometry, and that the deprotonated complexes assume a five-coordinated square pyramidal geometry exhibiting an axial coordination of the imidazolate nitrogen of the adjacent unit, as described by the X-ray structure analysis of **2′**. On the other hand, the d–d bands of **4** at 567 nm and **4′** at 566 nm showed no difference, indicating that **4** and **4′** assume a similar square-planar coordination geometry to each other, as elucidated by their X-ray analyses.

The solubility of the deprotonated compounds, which should be related to the dissociation from an infinite-chain polymeric structure with the imidazolate-bridges $\{-\mathrm{Cu(II)}-\mathrm{Im}\}_n$ to monomeric species, is influenced by both the steric effect of the substituent of the imidazole moiety and by the ligand field strength of the quadridentate ligand. The deprotonated complexes become soluble as the substituent of the imidazole moiety becomes sufficiently large and the ligand field strength of the quadridentate ligand increases, for example the order of the solubility in methanol: the deprotonated complex without the substituent of the imidazole moiety (insoluble in common solvents) $\ll$**1′** < **2′**; **1′** < **3′**; **2′** < **4′**. The d–d band maxima of **1′**, **2′**, and **3′** in methanol are 589, 598, 546 nm, respectively, whose values are different from those of the solid reflectance spectra of 653, 656, and 632 nm, respectively, and similar to those of the corresponding protonated complexes in methanol of 593, 601, and 549 nm, respectively. This fact indicates that the deprotonated self-assembled structures **1′** and **2′**, and **3′** dissociate from the self-assembled imidazolate-bridged one-dimensional chain structure with five-coordination number to monomeric species with four-coordination number. On the other hand, **4′** showed no assembly behavior, and exists as a monomer, even in the solid state, since **4′** has a bulky substituent and a strong enough ligand field to prevent the formation of an imidazolate bridge.

One can conclude the self-assembly property for this series of copper(II) complexes with quadridentate ligand is as follows. When the ligand field strength of the equatorial quadridentate ligand is sufficiently weak to receive the imidazolate nitrogen atom of the adjacent molecule at the vacant axial site, and when the self-assembly process is not prevented by the substituent of the 2-substituted-4-formylimidazole moiety, the rather stable self-assembled structure can form like in the case of (*N*-salicylidene-*N′*-(imidazolato-4-ylmethylidene)-1,3-propanediamine)copper(II),[7c)] where the complex has no substituent at the 2-position and has a weaker ligand field, and the deprotonated complex is insoluble in common solvents. These two effects work cooperatively and determine the self-assembly behavior.

Concluding Remarks. This series of studies was carried out in order to open up the chemistry of a self-assembly metal complex based on a new concept, and to develop a novel functional material exhibiting a switching ability. The copper(II) complexes with quadridentate ligands involving an imidazole moiety undergo to imidazolate-bridged infinite-chain polymers by deprotonation of the imidazole proton. The self-assembly behavior depends on both the steric-hindrance effect of the substituent and the ligand-field strength of the equatrial ligand. When the substituent of imidazole is sufficiently large, the deprotonated self-assembled compound tends to be soluble in solvents, accompanying the dissociation of the imidazolate-bridged polymer to a monomeric species. The resulting monomeric species can function as a ligand-complex and be useful for the syntheses of homo- and hetero-metal polynuclear complexes. A study along this line will be reported elsewhere.

Experimental

Warning: Perchlorate salts are potentially explosive and should only be handled in small quantities.

Materials. All chemicals and solvents used for the synthesis were of reagent grade and used as received. The reagents used for the physical measurements were of spectroscopic grade.

(*N*-Salicylidene-*N′*-(2-metylimidazol-4-ylmethylidene)-1,3-propanediamino)copper(II) Perchlorate $[\mathrm{CuHL^1}]\mathrm{ClO_4}$ 1. Bis(*N*-salicylidene-1,3-propanediaminato)nickel(II) was prepared by the method of Elder.[8)] To a nickel(II) complex (20 mmol) in methanol (100 ml) was added dimethylglyoxime (40 mmol); the mixture was refluxed for 1.5 h. After cooling to room temperature, thus precipitated red colored bis(dimetylglyoximato)nickel(II) was filtered off. To the filtrate was added 2-methyl-4-formylimidazole (40 mmol). The mixture was warmed in a water-bath at 50 °C for 30 min, and then cooled to room temperature. The resulting yellow solution was used in a subsequent reaction without isolating the quadridentate ligand. To a methanol solution of the ligand (40 mmol) was added copper(II) nitrate hexahydrate (40 mmol) in methanol; the mixture was then warmed for 10 min. The resulting mixture was filtered and the filtrate was allowed to stand for several days. Olive-green crystals thus precipitated were filtered off, washed with acetone and dried in vacuo. Recrystallization was carried out from the minimum amount of DMF and methanol at room temperature. $[CuHL^1]NO_3$; IR data (cm^{-1}) ν(N–H) = 3250, ν(C=N) = 1630, ν(N–O) = 1400. Found: C, 45.68; H, 4.12; N, 17.90; Cu, 16.11%. Calcd for $C_{15}H_{17}N_5O_4Cu$: C, 45.63; H, 4.34; N, 17.74; Cu, 16.09%. The perchlorate salt, $[CuHL^1]ClO_4$ **1**, was prepared by mixing of the nitrate salt and a slightly excess amount of sodium perchlorate in methanol.

(*N*-Salicylidene-*N*′-(2-phenylimidazol-4-ylmethylidene)-1,3-propanediamino)copper(II) Perchlorate $[CuHL^2]ClO_4$ 2. The ligand was prepared according to the same procedure as described for **1**, by using 2-phenyl-4-formylimidazole (40 mmol) instead of 2-methyl-4-formylimidazole. The resulting yellow solution containing the ligand was used in a subsequent reaction without isolation. The ligand solution was mixed with a solution of copper(II) perchlorate hexahydrate (40 mmol) in 20 ml of methanol. After standing overnight, olive-yellow crystals were collected by suction filtration, washed with a minimum amount of methanol and dried in vacuo. IR data (cm^{-1}) ν(N–H) = 3220, ν(C=N) = 1640, ν(Cl–O) = 1090. Found: C, 48.02; H, 4.22; N, 10.35; Cu, 12.40%. Calcd for $C_{20}H_{19}N_4O_5ClCu{\cdot}CH_3OH$: C, 47.91; H, 4.40; N, 10.64; Cu, 12.07%.

(*N*-Acetylacetonylidene-*N*′-(2-methylimidazol-4-ylmethylidene)ethylenediamino)copper(II) Perchlorate $[CuHL^3]ClO_4$ 3. A copper(II) complex with the half-unit ligand HL′ of the 1 : 1 condensation product of acetylacetone and ethylenediamine, [CuL′(acetato)], was prepared by the method of Costes.[9e)] To a solution of [CuL′(acetato)] (10 mmol) was added a methanol solution of 2-methyl-4-formylimidazole, the mixture was stirred for 30 min on a hot plate. To the resulting solution was added a solution of sodium perchlorate in methanol. After standing for several hours, dark red-purple crystals were precipitated, and collected by suction filtration, then dried in vacuo Recrystallization was carried out from methanol. IR data (cm^{-1}) ν(N–H) = 3200, ν(C=N) = 1640, ν(Cl–O) = 1090. Found: C, 36.23; H, 4.33; N, 13.99%. Calcd for $C_{12}H_{17}N_4O_5ClCu$: C, 36.37; H, 4.32; N, 14.14%.

(*N*-Acetylacetonylidene-*N*′-(2-phenylimidazol-4-ylmethylidene)ethylenediamino)copper(II) Perchlorate $[CuHL^4]ClO_4$ 4. The complex was prepared according to the same procedure as described for **3**, by using 2-phenyl-4-formylimidazole (40 mmol) instead of 2-methyl-4-formylimidazole. Dark violet-colored crystals. IR data (cm^{-1}) ν(N–H) = 3250, ν(C=N) = 1655, ν(Cl–O) = 1090. Found: C, 43.17; H, 4.16; N, 11.79%. Calcd for $C_{17}H_{19}N_4O_5ClCu{\cdot}H_2O$: C, 42.86; H, 4.44; N, 11.76%.

$[CuHL^2][Cu(saltn)]ClO_4$. During the course of the synthesis of **2**, a compound with the formula $[CuHL^2][Cu(saltn)]ClO_4$ was obtained as a small amount of the subproduct. A green-colored crystal was subjected to the single-crystal X-ray analysis.

$[CuL^1]_n$ 1′. The deprotonation reaction of the imidazole proton of **1** was carried out by either Method A or Method B.

Method A: The protonated complex **1** (10 mmol) was dissolved in a minimum amount of methanol. To the solution was added an excess amount of triethylamine. After stirring the mixture for several hours, bright-green crystals were precipitated, and collected by suction filtration, washed with ethanol and ether, and dried in vacuo. Recrystallization was carried out from methanol at room temperature. IR data (cm^{-1}) ν(C=N) = 1640. Found: C, 53.08; H, 4.95; N, 17.01; Cu, 18.81%. Calcd for $C_{15}H_{16}N_4OCu{\cdot}0.5H_2O$: C, 52.85; H, 5.03; N, 16.44; Cu, 18.64%.

Method B. The protonated complex **1** (10 mmol) was suspended in water and chloroform (30 ml each). To the suspension was added an aqueous solution of 1 M NaOH (10 mmol). After stirring the mixture for one hour at room temperature, a red-colored chloroform layer was collected and filtered. The chloroform solution was evaporated to dryness. During the reduction of the solution, green crystals were obtained. They were recrystallized from chloroform/methanol.

$[CuL^2]_n$ 2′. The complex can be prepared by either of Method A and Method B. Bright green crystals. IR data (cm^{-1}) ν(C=N) = 1640. Found: C, 58.90; H, 4.92; N, 13.11; Cu, 14.41%. Calcd for $C_{21}H_{22}N_4O_2Cu$: C, 59.21; H, 5.21; N, 13.15; Cu, 14.92%.

$[CuL^3]_n$ 3′. The complex was prepared by Method B. Blue-green crystals. IR data (cm^{-1}) ν(C=N) = 1625. Found: C, 47.51; H, 5.33; N, 18.31%. Calcd for $C_{12}H_{16}N_4OCu{\cdot}0.5H_2O$: C, 47.28; H, 5.62; N, 18.38%.

$[CuL^4]_n$ 4′. The complex was prepared by Method B. Dark-violet crystals. IR data (cm^{-1}) ν(C=N) = 1632. Found: C, 56.85; H, 5.09; N, 15.47%. Calcd for $C_{17}H_{18}N_4OCu$: C, 57.05; H, 5.07; N, 15.64%.

Physical Measurements. Elemental analyses for C, H, and N were performed at the Elemental Analysis Service Center of Kyushu University. Metal analyses were made on a Shimadzu AA-680 Atomic Absorption/Flame Emission Spectrophotometer. Infrared spectra were measured on KBr disks with a JASCO IR-810 spectrophotometer. Electrical-conductivity measurements were carried out on a Denki Kagaku Keiki AOL-10 digital conductometer in ca. 10^{-3} mol dm^{-3} solutions. The melting points were measured on a Yanagimoto micromelting points apparatus, and were uncorrected. Electronic spectra were measured on a Shimadzu MPS-2000 Multipurpose Recording Spectrophotometer. The magnetic susceptibilities were measured with a HOXAN HSM-D SQUID susceptometer in the temperature range 4.2—100 K and with a Faraday balance over the temperature range 80—300 K. The calibration was made with $Mn(NH_4)_2(SO_4)_2{\cdot}6H_2O$ for the SQUID susceptometer and with $[Ni(en)_3]S_2O_3$ for the Faraday balance. Diamagnetic corrections were made with Pascal's constants.[16)] Effective magnetic moments were calculated by the equation $\mu_{\rm eff} = 2.828(\chi_{\rm A}T)^{1/2}$, where $\chi_{\rm A}$ is the magnetic susceptibility.

Crystallographic Structure Determinations. The crystal of **2′** tends to decompose due to an elimination of the crystal solvent, so that it was encapsulated into a glass capillary with a small amount of the mother liquid. Except for **2′**, the crystals were mounted on a glass rod and coated with epoxy resin. All of the measurements were made on a Rigaku AFC7R diffractometer with graphite monochromated Mo $K\alpha$ radiation (λ = 0.71069 Å) and a 12 kW rotating-anode generator. The data were collected at a temperature of 20±1°C using the ω–2θ scan technique to a maximum 2θ value of 50.0° at a scan speed of 16.0° min^{-1} (in omega). The weak reflections ($I < 10.0\sigma(I)$) were rescanned (maximum of 4 scans) and the counts were accumulated to ensure good counting statistics. Stationary background counts were recorded on each side of the reflection. The ratio of the peak counting time to the background counting time was 2 : 1. The diameter of the incident beam collimator was 1.0 mm, the crystal to detector distance was 235 mm, and the computer controlled detector aperture was set to 9.0×13.0 mm (horizontal, vertical). The intensities of three representative reflections were measured after every 150 reflections. During the course of the data collection, the standards reflections were monitored and the decay corrections were applied by a polynomial correction. An empirical absorption correction based on azimuthal scans of several reflections was applied. The data were corrected for Lorentz and polarization effects.

Table 3. Crystallographic Data for [CuHL^1]ClO$_4$ **1**, [CuHL^3]ClO$_4$ **3**, [CuHL^4]ClO$_4$ **4**, and **2**·[Cu(saltn)]

Compound	[CuHL^1]ClO$_4$ **1**	[CuHL^3]ClO$_4$ **3**	[CuHL^4]ClO$_4$ **4**	**2**·[Cu(saltn)]
Formula	$C_{15}H_{17}N_4O_5ClCu$	$C_{12}H_{17}O_5N_4ClCu$	$C_{17}H_{19}O_5N_4ClCu$	$C_{37}H_{35}O_7N_6Cu_2Cl$
Formula weight	432.32	396.29	458.36	838.26
Crystal color	Olive green	Dark red purple	Dark violet	Bright green
Crystal system	Monoclinic	Monoclinic	Triclinic	Monoclinic
Space group	$P2_1/n$	$P2_1/a$	$P\bar{1}$	$P2_1/c$
a/Å	7.063(2)	9.178(8)	11.229(2)	13.032(4)
b/Å	19.735(3)	13.604(7)	11.985(4)	18.094(4)
c/Å	12.143(5)	13.16(1)	7.561(1)	15.214(3)
α/deg	90	90	97.56(2)	90
β/deg	96.38(3)	102.70(7)	99.10(2)	93.00(2)
γ/deg	90	90	108.56(1)	90
V/Å^3	1682.1(6)	1602(1)	934.2(4)	3582(1)
Z	4	4	2	4
D_{cal}/g cm^{-3}	1.707	1.642	1.629	1.554
F(000)	884.0	812.0	470.0	1720.0
Radiation	Mo$K\alpha$	Mo$K\alpha$	Mo$K\alpha$	Mo$K\alpha$
μ/cm^{-1}	14.94	15.59	13.49	13.21
No. of obsd ref.	3336	2129	2942	4101
R/%	6.5	6.4	4.7	8.6
R_w/%	5.8	6.8	4.7	7.2

Obsd ref. denote the reflections with $I > 3.0\sigma(I)$. $R=\sum||F_o|-|F_c||/\sum|F_o|$, $R_w=[\sum w(|F_o|-|F_c|)^2/\sum w|F_o|^2]^{1/2}$, $w=1/[\sigma(F_o)^2]$.

The structures were solved by direct methods and expanded using Fourier techniques.[17,18] The non-hydrogen atoms were refined anisotropically. Hydrogen atoms were included. Full-matrix least-squares refinement based on observed reflections were employed, where the unweighted and weighted agreement factors of $R=\sum||F_o|-|F_o||/\sum|F_o|$ and $R_w=[\sum w(|F_o|-|F_c|)^2/\sum w|F_o|^2]^{1/2}$ are used. The weighting scheme was based on counting statistics. Plots of $\sum w(|F_o|-|F_c|)^2$ versus $|F_o|$, reflection order in data collection, $\sin\theta/\lambda$ and various classes of indices showed no unusual

Table 4. Crystallographic Data for [CuL^2] **2′** and [CuL^4] **4′**

Compound	[CuL^2] **2′**	[CuL^4] **4′**
Formula	$C_{41}H_{42}N_8O_4Cu_2$	$C_{17}H_{18}N_4OCu$
Formula weight	837.9	357.9
Crystal color	Bright green	Dark red purple
Crystal system	Monoclinic	Triclinic
Space group	$P2_1/n$	$P\bar{1}$
a/Å	14.762(8)	10.401(3)
b/Å	17.901(5)	10.565(2)
c/Å	15.750(5)	7.332(2)
α/deg	90	91.72(2)
β/deg	106.50(3)	96.65(2)
γ/deg	90	74.57(2)
V/Å^3	3390(2)	771.5(3)
Z	4	2
D_{cal}/g cm^{-3}	1.395	1.541
F(000)	1736	370
Radiation	Mo$K\alpha$	Mo$K\alpha$
μ/cm^{-1}	11.17	14.25
No. of reflections	7587	2885
No. of obsd refl.	4613	2441
R/%	5.0	2.6
R_w/%	5.0	2.2

Obsd ref. denote the reflections with $I > 3.0\sigma(I)$.
$R=\sum||F_o|-|F_c||/\sum|F_o|$, $R_w=[\sum w(|F_o|-|F_c|)^2/\sum w|F_o|^2]^{1/2}$, $w=1/[\sigma(F_o)^2]$.

Table 5. Atomic Coordinates and Equivalent Isotropic Thermal Parameters of Non-Hydrogen for [CuHL^1]ClO$_4$ **1**

Atom	x	y	z	B_{eq}/Å^2
Cu1	0.2688(1)	0.03556(5)	−0.05590(7)	0.0357
Cl1	0.2434(3)	0.18081(10)	0.4392(2)	0.0470
O1	0.3200(7)	−0.0448(2)	0.0290(4)	0.0417
O2	0.395(2)	0.1431(6)	0.4763(8)	0.2076
O3	0.103(2)	0.1374(6)	0.4277(9)	0.2214
O4	0.275(2)	0.2036(4)	0.3419(6)	0.1877
O5	0.2217(10)	0.2297(3)	0.5213(5)	0.0832
N1	0.3607(9)	−0.0688(3)	−0.3466(5)	0.0371
N2	0.3019(8)	−0.0142(3)	−0.1981(5)	0.0208
N3	0.2492(8)	0.1153(3)	−0.1605(5)	0.0258
N4	0.1850(8)	0.0873(3)	0.0683(5)	0.0259
C1	0.332(1)	−0.1401(4)	−0.1851(6)	0.0496
C2	0.3332(10)	−0.0739(4)	−0.2391(6)	0.0299
C3	0.344(1)	−0.0025(4)	−0.3756(6)	0.0467
C4	0.3081(10)	0.0309(4)	−0.2832(6)	0.0350
C5	0.277(1)	0.1015(4)	−0.2573(6)	0.0367
C6	0.218(1)	0.1872(4)	−0.1350(6)	0.0453
C7	0.256(1)	0.2003(4)	−0.0103(6)	0.0507
C8	0.124(1)	0.1598(4)	0.0548(6)	0.0480
C9	0.170(1)	0.0620(4)	0.1630(6)	0.0398
C10	0.204(1)	−0.0078(4)	0.1980(6)	0.0360
C11	0.163(1)	−0.0256(4)	0.3066(6)	0.0418
C12	0.186(1)	−0.0911(4)	0.3441(6)	0.0460
C13	0.248(1)	−0.1402(4)	0.2746(6)	0.0448
C14	0.287(1)	−0.1251(4)	0.1701(6)	0.0366
C15	0.272(1)	−0.0575(4)	0.1282(6)	0.0376

$B_{eq}=(8\pi^2/3)(U_{11}(aa^*)^2+U_{22}(bb^*)^2+U_{33}(cc^*)^2$
$+2U_{12}aa^*bb^*\cos\gamma+2U_{13}aa^*cc^*\cos\beta+2U_{23}bb^*cc^*\cos\alpha)$.

Table 6. Atomic Coordinates and Equivalent Isotropic Thermal Parameters of Non-Hydrogen for [CuHL^3]ClO$_4$
3

Atom	x	y	z	B_{eq}/Å^2
Cu1	0.1151(1)	0.21331(7)	−0.21326(8)	0.0423(3)
Cl1	1.0109(3)	0.3297(2)	0.3801(2)	0.0586(7)
O1	0.2720(6)	0.1672(4)	−0.1063(5)	0.051(2)
O2	0.990(1)	0.3008(7)	0.2778(7)	0.119(4)
O3	0.878(1)	0.3685(7)	0.3961(10)	0.136(4)
O4	1.129(1)	0.3980(6)	0.4015(8)	0.111(3)
O5	1.0512(8)	0.2477(4)	0.4491(6)	0.075(2)
N1	−0.0303(9)	−0.0560(5)	−0.3536(7)	0.063(3)
N2	0.0433(7)	0.0846(4)	−0.2810(5)	0.042(2)
N3	−0.0479(8)	0.2615(5)	−0.3214(6)	0.047(2)
N4	0.1624(8)	0.3517(4)	−0.1937(6)	0.047(2)
C1	0.185(1)	−0.0645(6)	−0.2001(9)	0.064(3)
C2	0.0689(10)	−0.0126(6)	−0.2761(8)	0.049(3)
C3	−0.124(1)	0.0129(7)	−0.4103(8)	0.066(3)
C4	−0.0759(10)	0.1005(6)	−0.3643(7)	0.051(3)
C5	−0.1215(9)	0.2019(6)	−0.3861(7)	0.050(3)
C6	−0.066(1)	0.3686(6)	−0.3282(9)	0.069(3)
C7	0.054(1)	0.4161(7)	−0.257(1)	0.094(4)
C8	0.2844(9)	0.3837(6)	−0.1319(7)	0.047(3)
C9	0.313(1)	0.4947(6)	−0.1214(9)	0.066(3)
C10	0.3901(9)	0.3226(6)	−0.0695(7)	0.050(3)
C11	0.3792(9)	0.2215(6)	−0.0564(7)	0.047(2)
C12	0.498(1)	0.1706(8)	0.0226(8)	0.063(3)

$B_{eq}=(8\pi^2/3)(U_{11}(aa^*)^2+U_{22}(bb^*)^2+U_{33}(cc^*)^2$
$+2U_{12}aa^*bb^*\cos\gamma+2U_{13}aa^*cc^*\cos\beta+2U_{23}bb^*cc^*\cos\alpha)$.

Table 7. Atomic Coordinates and Equivalent Isotropic Thermal Parameters of Non-Hydrogen for [CuHL^4]ClO$_4$
4

Atom	x	y	z	B_{eq}/Å^2
Cu1	0.10991(5)	0.22271(5)	−0.07746(8)	0.0441
Cl1	0.6164(1)	0.2907(1)	0.3840(2)	0.0632
O1	−0.0697(3)	0.1562(3)	−0.1475(4)	0.0539
O2	0.7391(3)	0.2837(3)	0.4569(5)	0.0760
O3	0.6351(5)	0.3859(5)	0.2888(8)	0.1455
O4	0.5587(4)	0.3104(5)	0.5307(7)	0.1360
O5	0.5387(4)	0.1817(4)	0.2614(6)	0.0972
N1	0.2342(4)	−0.0602(4)	−0.3013(6)	0.0530
N2	0.1634(3)	0.0796(3)	−0.1885(5)	0.0401
N3	0.2936(4)	0.3036(4)	−0.0215(5)	0.0509
N4	0.1107(4)	0.3673(3)	0.0730(5)	0.0458
C1	−0.1097(4)	−0.1004(4)	−0.3025(7)	0.0550
C2	−0.2313(5)	−0.1791(5)	−0.3763(8)	0.0588
C3	−0.2507(5)	−0.2818(5)	−0.4983(7)	0.0523
C4	−0.1448(4)	−0.3016(4)	−0.5463(6)	0.0486
C5	−0.0238(4)	−0.2234(4)	−0.4762(6)	0.0467
C6	−0.0035(4)	−0.1208(4)	−0.3536(6)	0.0395
C7	0.1272(4)	−0.0327(4)	−0.2793(6)	0.0414
C8	0.3394(4)	0.0357(5)	−0.2239(8)	0.0594
C9	0.2979(4)	0.1222(4)	−0.1545(7)	0.0466
C10	0.3631(4)	0.2437(5)	−0.0629(7)	0.0537
C11	0.3376(5)	0.4310(5)	0.0633(8)	0.0725
C12	0.2397(5)	0.4553(5)	0.1559(7)	0.0597
C13	0.0100(5)	0.3817(4)	0.1244(6)	0.0480
C14	0.0221(5)	0.4879(5)	0.2658(7)	0.0647
C15	−0.1162(5)	−0.2998(5)	0.0484(7)	0.0501
C16	−0.1496(5)	0.1979(5)	−0.0803(7)	0.0495
C17	−0.2882(5)	−0.1226(5)	−0.1565(8)	0.0680

$B_{eq}=(8\pi^2/3)(U_{11}(aa^*)^2+U_{22}(bb^*)^2+U_{33}(cc^*)^2$
$+2U_{12}aa^*bb^*\cos\gamma+2U_{13}aa^*cc^*\cos\beta+2U_{23}bb^*cc^*\cos\alpha)$.

Table 8. Atomic Coordinates and Equivalent Isotropic Thermal Parameters of Non-Hydrogen for **2**·[Cu(saltn)]ClO$_4$

Atom	x	y	z	B_{eq}/Å^2
Cu1	0.4301(1)	0.13079(8)	−0.05053(9)	0.0376
Cu2	0.21365(10)	0.18961(8)	−0.16125(8)	0.0341
Cl	0.7860(4)	0.3525(3)	0.1397(4)	0.0741
O1	0.2923(6)	0.0969(5)	−0.0453(4)	0.0704
O2	0.3549(5)	0.2227(4)	−0.1534(4)	0.0636
O3	0.2714(5)	0.1260(4)	−0.2458(5)	0.0362
O4	0.8128(9)	0.4176(8)	0.1789(9)	0.1820
O5	0.842(2)	0.3290(7)	0.087(1)	0.3320
O6	0.704(1)	0.3724(9)	0.088(1)	0.1652
O7	0.753(1)	0.3037(9)	0.1947(9)	0.2839
N1	0.3833(7)	0.2905(5)	0.1455(5)	0.0446
N2	0.4148(7)	0.1989(5)	0.0543(5)	0.0513
N3	0.5705(7)	0.1764(6)	−0.0463(7)	0.0683
N4	0.4687(8)	0.0522(8)	−0.1318(6)	0.0655
N5	0.1691(8)	0.2778(8)	−0.0938(6)	0.0563
N6	0.0741(7)	0.1452(6)	−0.1789(7)	0.0508
C1	0.4750(9)	0.3057(7)	0.1132(7)	0.0472
C2	0.4965(8)	0.2492(7)	0.0567(7)	0.0470
C3	0.5789(9)	0.2320(8)	0.0044(8)	0.0549
C4	0.6576(9)	0.1591(9)	−0.1023(8)	0.0731
C5	0.656(1)	0.083(1)	−0.133(1)	0.0873
C6	0.0565(1)	0.0644(8)	−0.1846(9)	0.1020
C7	0.415(1)	−0.0062(9)	−0.1444(9)	0.0556
C8	0.318(1)	−0.0234(7)	−0.1117(7)	0.0559
C9	0.273(2)	−0.0927(8)	−0.1309(9)	0.0700
C10	0.180(2)	−0.1120(9)	−0.105(1)	0.1022
C11	0.122(1)	−0.062(1)	−0.0597(10)	0.0751
C12	0.162(1)	0.0092(7)	−0.0395(7)	0.0620
C13	0.260(1)	0.0293(7)	−0.0653(7)	0.0430
C14	0.3476(9)	0.2250(6)	0.1104(7)	0.0378
C15	0.2535(9)	0.1908(7)	0.1377(6)	0.0461
C16	0.1660(10)	0.2325(6)	0.1498(7)	0.0522
C17	0.0800(9)	0.2001(9)	0.1809(8)	0.0572
C18	0.080(1)	0.126(1)	0.2024(8)	0.0685
C19	0.167(2)	0.0845(8)	0.1925(8)	0.0759
C20	0.253(1)	0.1156(7)	0.1600(8)	0.0639
C21	0.3879(10)	0.2933(7)	−0.1436(7)	0.0430
C22	0.4854(10)	0.3125(7)	−0.1710(7)	0.0704
C23	0.526(1)	0.382(1)	−0.155(1)	0.0893
C24	0.468(2)	0.435(1)	−0.114(1)	0.0907
C25	0.371(2)	0.4191(8)	−0.0916(9)	0.0772
C26	0.328(1)	0.3477(8)	−0.1061(8)	0.0507
C27	0.225(1)	0.3356(9)	−0.0819(8)	0.0582
C28	0.065(1)	0.2860(9)	−0.0621(9)	0.0802
C29	0.007(1)	0.219(1)	−0.065(1)	0.3058
C30	−0.013(1)	0.1668(9)	−0.1275(10)	0.0683
C31	0.0513(9)	0.0946(8)	−0.2374(10)	0.0534
C32	0.1153(10)	0.0599(7)	−0.2958(8)	0.0554
C33	0.071(1)	0.0075(8)	−0.355(1)	0.0690
C34	0.127(2)	−0.0307(8)	−0.4135(10)	0.0975
C35	0.232(1)	−0.0182(7)	−0.4138(9)	0.0773
C36	0.2775(9)	0.0333(7)	−0.3573(9)	0.0578
C37	0.2247(9)	0.0776(7)	−0.2950(8)	0.0759

$B_{eq}=(8\pi^2/3)(U_{11}(aa^*)^2+U_{22}(bb^*)^2+U_{33}(cc^*)^2$
$+2U_{12}aa^*bb^*\cos\gamma+2U_{13}aa^*cc^*\cos\beta+2U_{23}bb^*cc^*\cos\alpha)$.

Table 9. Atomic Coordinates and Equivalent Isotropic Thermal Parameters of Non-Hydrogen for [CuL^2] **2′**

Atom	x	y	z	B_{eq}/Å^2
Cu1	0.16695(7)	0.01871(5)	0.09544(6)	0.0396(3)
Cu2	0.44562(7)	−0.11707(5)	0.44289(6)	0.0419(3)
O1	0.2137(4)	0.0356(3)	−0.0057(3)	0.047(2)
O2	0.5390(4)	−0.1151(3)	0.3809(3)	0.049(2)
O3	0.2206(9)	0.2072(6)	0.8704(6)	0.304(7)
O4	1.001(1)	0.0356(8)	0.3856(8)	0.287(8)
N1	0.1045(4)	0.2529(3)	0.0935(4)	0.042(2)
N2	0.1436(4)	0.1307(3)	0.1074(4)	0.034(2)
N3	0.0476(4)	0.0120(3)	0.1381(4)	0.042(2)
N4	0.1648(4)	−0.0907(3)	0.0781(4)	0.044(2)
N5	0.2757(4)	0.0054(3)	0.2256(4)	0.041(2)
N6	0.3558(4)	−0.0655(3)	0.3409(4)	0.037(2)
N7	0.3572(4)	−0.0710(3)	0.5071(4)	0.044(2)
N8	0.5388(5)	−0.1418(3)	0.5530(4)	0.043(2)
C1	0.2696(5)	0.2194(4)	0.1002(5)	0.040(2)
C2	0.3366(6)	0.1663(4)	0.1020(6)	0.054(3)
C3	0.4302(6)	0.1852(5)	0.1100(6)	0.057(3)
C4	0.4569(6)	0.2591(6)	0.1173(6)	0.064(3)
C5	0.3916(7)	0.3128(5)	0.1158(7)	0.077(4)
C6	0.2989(6)	0.2924(5)	0.1089(7)	0.064(3)
C7	0.1717(5)	0.2005(4)	0.0967(5)	0.034(2)
C8	0.0288(5)	0.2151(4)	0.1055(5)	0.042(3)
C9	0.0532(5)	0.1402(4)	0.1144(5)	0.037(2)
C10	0.0071(5)	0.0760(5)	0.1352(5)	0.042(3)
C11	0.0078(6)	−0.0517(4)	0.1718(6)	0.054(3)
C12	0.0280(7)	−0.1236(5)	0.1314(6)	0.064(3)
C13	0.1317(7)	−0.1372(4)	0.1393(6)	0.057(3)
C14	0.1957(6)	−0.1244(4)	0.0208(5)	0.048(3)
C15	0.2339(5)	−0.0916(4)	−0.0449(5)	0.043(3)
C16	0.2654(6)	−0.1398(5)	−0.1004(6)	0.061(3)
C17	0.3057(7)	−0.1145(6)	−0.1632(6)	0.072(4)
C18	0.3147(7)	−0.0373(6)	−0.1708(6)	0.080(4)
C19	0.2848(6)	0.0109(5)	−0.1176(6)	0.063(3)
C20	0.2415(5)	−0.0127(5)	−0.0537(5)	0.044(3)
C21	0.3901(5)	−0.0873(4)	0.1991(5)	0.041(2)
C22	0.4061(6)	−0.1636(5)	0.2082(5)	0.048(3)
C23	0.4525(7)	−0.2018(5)	0.1563(6)	0.062(3)
C24	0.4850(7)	−0.1636(6)	0.0952(7)	0.073(4)
C25	0.4692(6)	−0.0875(6)	0.0845(6)	0.068(4)
C26	0.4223(6)	−0.0494(4)	0.1365(6)	0.051(3)
C27	0.3411(5)	−0.0484(4)	0.2556(5)	0.037(2)
C28	0.2463(5)	0.0228(4)	0.2970(5)	0.044(2)
C29	0.2951(5)	−0.0192(4)	0.3683(5)	0.038(2)
C30	0.2971(5)	−0.0259(4)	0.4587(5)	0.043(3)
C31	0.3586(6)	−0.0799(5)	0.5988(6)	0.062(3)
C32	0.4580(7)	−0.0911(5)	0.6572(5)	0.059(3)
C33	0.5055(6)	−0.1593(5)	0.6307(6)	0.062(3)
C34	0.6278(6)	−0.1579(4)	0.5623(5)	0.048(3)
C35	0.6757(6)	−0.1511(4)	0.4967(6)	0.043(3)
C36	0.7726(7)	−0.1633(5)	0.5214(6)	0.061(3)
C37	0.8249(7)	−0.1563(6)	0.4623(8)	0.079(4)
C38	0.7800(7)	−0.1370(5)	0.3755(8)	0.076(4)
C39	0.6842(6)	−0.1247(5)	0.3494(6)	0.059(3)
C40	0.6288(6)	−0.1301(4)	0.4085(6)	0.045(3)
C41	0.900(1)	0.080(1)	0.382(1)	0.24(1)

$B_{eq}=(8\pi^2/3)(U_{11}(aa^*)^2+U_{22}(bb^*)^2+U_{33}(cc^*)^2+2U_{12}aa^*bb^*\cos\gamma+2U_{13}aa^*cc^*\cos\beta+2U_{23}bb^*cc^*\cos\alpha)$.

Table 10. Atomic Coordinates and Equivalent Isotropic Thermal Parameters of Non-Hydrogen for [CuL^4] **4′**

Atom	x	y	z	B_{eq}/Å^2
Cu1	0.38708(3)	0.08941(3)	0.30671(4)	0.0390
O1	0.2060(2)	0.0979(2)	0.3184(2)	0.0509
N1	0.5349(2)	−0.2938(2)	0.0534(3)	0.0503
N2	0.4518(2)	−0.0953(2)	0.1856(3)	0.0366
N3	0.5733(2)	0.0864(2)	0.3082(3)	0.0417
N4	0.3735(2)	0.2644(2)	0.4113(3)	0.0401
C1	0.1785(3)	−0.1556(3)	0.1260(4)	0.0559
C2	0.0617(3)	−0.1954(3)	0.1160(5)	0.0702
C3	0.0629(4)	−0.3239(4)	0.0804(5)	0.0730
C4	0.1820(4)	−0.4119(3)	0.0561(5)	0.0716
C5	0.2991(3)	−0.3747(3)	0.0665(4)	0.0549
C6	0.2996(2)	−0.2449(2)	0.1039(3)	0.0398
C7	0.4276(2)	−0.2085(2)	0.1159(3)	0.0393
C8	0.6323(3)	−0.2313(3)	0.0833(4)	0.0526
C9	0.5856(2)	−0.1116(2)	0.1637(3)	0.0404
C10	0.6460(3)	−0.0111(3)	0.2309(4)	0.0460
C11	0.6161(3)	0.1979(3)	0.3906(4)	0.0503
C12	0.4941(3)	0.3116(3)	0.4063(4)	0.0511
C13	0.2667(3)	0.3402(2)	0.4711(3)	0.0435
C14	0.2663(4)	0.4746(3)	0.5509(6)	0.0618
C15	0.1453(3)	0.3034(3)	0.4648(4)	0.0483
C16	0.1204(2)	0.1917(2)	0.3899(3)	0.0421
C17	−0.0181(3)	0.1711(4)	0.3839(6)	0.0587

$B_{eq}=(8\pi^2/3)(U_{11}(aa^*)^2+U_{22}(bb^*)^2+U_{33}(cc^*)^2+2U_{12}aa^*bb^*\cos\gamma+2U_{13}aa^*cc^*\cos\beta+2U_{23}bb^*cc^*\cos\alpha)$.

trends.

Neutral atom scattering factors were taken from Cromer and Waber. Anomalous dispersion effects were included in F_{calcd}; the values $\Delta f'$ and $\Delta f''$ were those of Creagh and McAuley.[19] The values for the mass attenuation coefficients are those of Creagh and Hubbel.[19] All calculations were performed using the teXsan crystallographic software package of Molecular Structure Corporation.[20]

The crystal data and details of the structure determination for the protonated complexes and the deprotonated complexes are summarized in Tables 3 and 4, respectively. The atomic coordinates of non-hydrogen atoms for six compounds (**1**, **3**, **4**, **2** [Cu(saltn)]ClO$_4$, **2′**, and **4′**) are given in Tables 5, 6, 7, 8, 9, and 10, respectively. The atomic coordinates, thermal parameters, bond distances and angles, and F_o-F_c tables were deposited as Document No. 70036 at the Office of the Editor of Bull. Chem. Soc. Jpn.

NM would like to express his sincere thanks to Dr. J.-P. Costes for the discussion of the synthetic procedure. We thank the Ministry of Education, Science, Sports and Culture for giving a Grant-in-Aid for Scientific Research Nos. 04453048 and 09874145.

References

1) J.-M. Lehn, "Supramolecular Chemistry," VCH (1995).

2) a) J.-M. Lehn, *Angew. Chem., Int. Ed. Engl.*, **102**, 1347 (1990); b) J.-M. Lehn, *J. Coord. Chem.*, **27**, 3 (1992); c) O. J. Gelling, F. Bolhuis, and B. L. Fering, *J. Chem. Soc., Chem. Commun.*, **1991**, 917; d) E. C. Constable, *Nature*, **346**, 314 (1990); e) E. C. Constable, *Tetrahedron*, **48**, 10013 (1992); f) D. M. L. Goodgame, D. J. Williams, and R. E. P. Winpenny, *J. Chem. Soc., Dalton Trans.*, **1991**, 917; g) R. F. Carina, G. Bernardinelli, and A.

F. Williams, *Angew. Chem., Int. Ed. Engl.*, **32**, 1463 (1993); h) P. Baxter, J.-M. Lehn, A. D. Cian, and J. Fischer, *Angew. Chem., Int. Ed. Engl.*, **32**, 69 (1993); i) P. R. Ashton, D. Philip, N. Spencer, and J. F. Stoddart, *J. Chem. Soc., Chem. Commun.*, **1992**, 1124.

3) a) E. C. Constable, A. J. Edwards, P. R. Raithby, and J. V. Walker, *Angew. Chem., Int. Ed. Engl.*, **32**, 1465 (1993); b) E. C. Constable, M. J. Hannon, and D. A. Tocher, *J. Chem. Soc., Dalton Trans.*, **1993**, 1883; c) E. C. Constable and R. Chotalia, *J. Chem. Soc., Chem. Commun.*, **1992**, 64; d) E. C. Constable, S. M. Elder, J. Healy, and M. D. Ward, *J. Am. Chem. Soc.*, **112**, 4590 (1990); e) E. C. Constable and M. D. Ward, *J. Am. Chem. Soc.*, **112**, 1256 (1990); f) S. Ruttimann, G. Bernardinelli, and A. F. Williams, *Angew. Chem., Int. Ed. Engl.*, **32**, 392 (1993); g) S. Ruttimann, C. Piguet, G. Bernardinelli, B. Bocquet, A. Quattropani, and A. F. Williams, *J. Am. Chem. Soc.*, **114**, 7440 (1992); h) L. J. Charbonniere, G. Bernardinelli, C. Piguet, A. M. Sargeson, and A. F. Williams, *J. Chem. Soc., Chem. Commun.*, **1994**, 1419; i) T. Kajiwara and T. Ito, *J. Chem. Soc., Chem. Commun.*, **1994**, 1773; j) Y. Nakano, W. Mori, N. Okuda, and A. Nakahara, *Inorg. Chim. Acta*, **35**, 1 (1979).

4) a) J.-M. Lehn, *Angew. Chem., Int. Ed. Engl.*, **29**, 1304 (1990); b) R. Kramer, J.-M. Lehn, A. D. Cian, and J. Fischer, *Angew. Chem., Int. Ed. Engl.*, **32**, 703 (1993).

5) a) J.-M. Lehn, A. Rigauld, J. Siegel, J. Harrowfield, B. Chevrier, and D. Moras, *Proc. Natl. Acad. Sci. U.S.A.*, **84**, 2565 (1987); b) A. Pfeil and J.-M. Lehn, *J. Chem. Soc., Chem. Commun.*, **1992**, 838.

6) a) N. Matsumoto, Y. Mizuguchi, G. Mago, S. Eguchi, H. Miyasaka, T. Nakashima, and J. P. Tuchagues, *Angew. Chem., Int. Ed. Engl.*, 1997, in press; b) N. Matsumoto, T. Nozaki, H. Usio, K. Motoda, M. Ohba, G. Mago, and H. Ōkawa, *J. Chem. Soc., Dalton Trans.*, **1993**, 2157; c) N. Matsumoto, S. Yamashita, A. Ohyoshi, S. Kohata, and H. Ōkawa, *J. Chem. Soc., Dalton Trans.*, **1988**, 1943; d) T. Nozaki, H. Ushio, G. Mago, N. Matsumoto, H. Ōkawa, Y. Yamakawa, T. Anno, and T. Nakashima, *J. Chem. Soc., Dalton Trans.*, **1994**, 2339.

7) a) N. Matsumoto, M. Ohba, M. Mitsumi, K. Inoue, Y. Hashimoto, and H. Ōkawa, *Mol. Cryst. Liq. Cryst.*, **233**, 299 (1993); b) N. Matsumoto, T. Akui, H. Murakami, J. Kanesaka, A. Ohyoshi, and H. Ōkawa, *J. Chem. Soc., Dalton Trans.*, **1988**, 1021; c) N. Matsumoto, H. Ōkawa, S. Kida, T. Ogawa, and A. Ohyoshi, *Bull. Chem. Soc. Jpn.*, **62**, 3812 (1989); d) T. Nozaki, N. Matsumoto, H. Okawa, H. Miyasaka, and G. Mago, *Inorg. Chem.*, **34**, 2108 (1995); e) N. Matsumoto, H. Tamaki, K. Inoue, M. Koikawa, Y. Maeda, H. Okawa, and S. Kida, *Chem. Lett.*, **1991**, 1393; f) K. Inoue, N. Matsumoto, and H. Okawa, *Chem. Lett.*, **1993**, 1433; g) C. T. Brewer and G. Brewer, *J. Chem. Soc., Dalton Trans.*, **1992**, 1669; h) C. T. Brewer, G. Brewer, L. Mat, J. Sitar, and R. Wang, *J. Chem. Soc., Dalton Trans.*, **1993**, 151.

8) R. C. Elder, *Aust. J. Chem.*, **31**, 35 (1978).

9) a) J.-P. Costes, F. Dahan, and J.-P. Laurent, *J. Chem. Soc., Dalton Trans.*, **1989**, 1017; b) J.-P. Costes and M. I. F-Garcis, *Inorg. Chim. Acta*, **237**, 57 (1995); c) J.-P. Costes, J. F. Serra, F. Dahan, and J.-P. Laurent, *Inorg. Chem.*, **25**, 2790 (1986); d) J.-P. Costes, G. Commenges, and J.-P. Laurent, *Inorg. Chim. Acta*, **134**, 237 (1987); e) J.-P. Costes, F. Dahan, and J.-P. Laurent, *Inorg. Chem.*, **24**, 1018 (1985).

10) a) J. P. Costes, *Bull. Soc. Chim. Fr.*, **1986**, 78; b) J. P. Costes, private communication.

11) K. Nakamoto, "Infrared and Raman Spectra of Inorganic and Coordination Compound," 3rd ed, John Wiley & Sons, New York (1978).

12) W. J. Geary, *Coord. Chem. Rev.*, **7**, 81 (1971).

13) E. Sinn, *Coord. Chem. Rev.*, **5**, 313 (1970).

14) O. Kahn, "Molecular Magnetism," VCH (1993).

15) L. F. Lindoy, V. Katovic, and D. H. Busch, *J. Chem. Educ.*, **49**, 117 (1972).

16) E. A. Boudreaux and L. N. Mulay, in "Theory and Applications of Molecular Paramagnetism," John Wiley and Sons, New York (1976), pp. 491—495.

17) SAPI91: Fan Hai-Fu (1991). "Structure Analysis Programs with Intelligent Control," Rigaku Corporation, Tokyo, Japan. MULTAN88: T. Debaerdemaeker, G. Germain, P. Main, L. S. Refaat, C. Tate, and M. M. Woolfson (1988); "Computer program for the automatic solution of crystal structures from X-ray diffraction data," University of York, U. K.; SHELXS86: G. M. Sheldrick, (1986). "A program for X-ray crystal structure determination," University of Cambridge.

18) DIRDIF92: P. T. Beurskens, G. Admiraal, G. Beurskens, W. P. Bosman, S. Garcia-Granda, R. O. Gould, J. M. M. Smits, and C. Smykalla (1992); "The DIRDIF Program System, Technical Report of the Crystallography Laboratory," University of Nijmegen, The Netherlands.

19) D. C. Creagh and W. J. McAuley, "International Tables for Crystallography," Vol. C, ed by A. J. C. Wilson, Kluwer Academic Publishers, Boston (1992); D. T. Cromer and J. T. Waber, "International Tables for X-Ray Crystallography," The Kynoch Press, Birmingham, England (1974), Vol. IV.

20) "teXsan: Crystal Structure Analysis Package," Molecular Structure Corporation (1985 & 1992).